

RSC Advances



This is an *Accepted Manuscript*, which has been through the Royal Society of Chemistry peer review process and has been accepted for publication.

Accepted Manuscripts are published online shortly after acceptance, before technical editing, formatting and proof reading. Using this free service, authors can make their results available to the community, in citable form, before we publish the edited article. This *Accepted Manuscript* will be replaced by the edited, formatted and paginated article as soon as this is available.

You can find more information about *Accepted Manuscripts* in the [Information for Authors](#).

Please note that technical editing may introduce minor changes to the text and/or graphics, which may alter content. The journal's standard [Terms & Conditions](#) and the [Ethical guidelines](#) still apply. In no event shall the Royal Society of Chemistry be held responsible for any errors or omissions in this *Accepted Manuscript* or any consequences arising from the use of any information it contains.

Cite this: DOI: 10.1039/c0xx00000x

www.rsc.org/xxxxxx

ARTICLE TYPE

UV-assisted size sampling and antibacterial screening of *Lantana camara* leaf extract synthesized silver nanoparticles

Pradeep Kumar Singh^{a,b}, Kirti Bhardwaj,^b Parul Dubey,^a Asmita Prabhune^{a*}⁵ Received (in XXX, XXX) Xth XXXXXXXXX 20XX, Accepted Xth X

XXXXXXX 20XX

DOI: 10.1039/b000000x

Green route synthesized silver nanoparticles are extremely toxic to multidrug resistant bacteria and have widespread applications in biomedical science. If the silver reducing weed extract possesses antimicrobial properties then it can additionally contribute to the medicinal activity. Herein, we present a synthesis of silver nanoparticles by using weed plant *Lantana camara*'s leaf extract. This study shows an easy, quick and cost-effective route to silver nanoparticle synthesis. Size control synthesis of Ag⁰ nanoparticles is studied and discussed based on optical absorption, photoluminescence, dynamic light scattering (DLS), zeta potential, infrared spectroscopy, X-ray diffraction measurements, FE-SEM and TEM analysis. The synthesis of silver nanoparticles via this green approach shows very high antibacterial activity against *E coli* (gram -ve) and *S aureus* (gram +ve) bacteria at a very low concentration (50 ppm Ag nanoparticles). Use of such eco-friendly nanoparticles may open a door for a new range of bactericidal agents.

Introduction

There are several reports on synthesis of silver nanoparticles using plants as the green reducing sources. However owing to the diversity of the plant kingdom, many systems and phenomena remain unexplored. Plant extract-driven green synthesis of silver nanoparticles has been studied using variety of plants like *Glycine max*,¹ *Cinnamon zeylanicum*,² *Camellia sinensis*³ and *Azadirachta indica*.⁴ The benefits of green route are that it offers cost effective, environment friendly⁵, and scalable options as compared to the established chemical and physical methods. Furthermore, the green synthesis route is advantageous as it does not involve use of toxic chemicals, high temperature, high pressure and energy. Presently however, chemical and physical methods are mainly employed.

Asmita Prabhune Corresponding-Author,

E-mail: aa.prabhune@ncl.res.in

^aBiochemical Sciences Division, National Chemical Laboratory (NCL), Council of Scientific and Industrial Research (CSIR), Dr. HomiBhabha Road, Pashan, Pune 411008, India

^bPhysical and Materials Chemistry Division, National Chemical Laboratory (NCL), Council of Scientific and Industrial Research (CSIR), Dr. HomiBhabha Road, Pashan, Pune 411008, India

Electronic Supplementary Information (ESI) available: [details of any supplementary information available should be included here]. See DOI: 10.1039/b000000x/

Despite that, there is persistent requirement for a commercially viable, economic and environment friendly route to silver nanoparticle synthesis.⁶⁻⁸ Silver nanoparticles find applications in disease prevention⁹⁻¹⁰, material chemistry, electronics, catalysis,¹¹ and plasmonics. These applications greatly depend upon the controlled size of silver nanoparticles and their assemblies. Quick and green synthesis is important to reduce investment and plan ecological costs for large scale production. Currently, large scale production involves chemical reactions in laboratories on a batch-scale.¹² A few reports have made practical progress in the direction of cost effective nanoparticle synthesis by using bio-derived compound like plant extracts and polysaccharides of biomaterials.¹³ Presently, green route synthesis reactions at room temperature take several hours for completion and are therefore not suited for bulk production.

*Lantana camara*¹⁴, a decorative garden plant is also considered as a notorious weed (Fig. 1A). It has various worldwide applications in the biomedical field. It is also identified as 'Spanish Flag', 'Wild Sage', 'Ghaneri'. This herb has recently been recognized for its natural health care potential aimed at restoring and protecting health. It acts as antibacterial and antifungal agent and is also used in HIV patients for boosting of immune system. It also acts as potential anti-tumor agents due to the presence of flavonoids and phenylpropanoid.¹⁵⁻¹⁶ Glycosides extracted from *Lantana camara* leaves have been reported to show significant hypoglycemic effect in mice.¹⁷⁻¹⁹ Its methanolic extracts are active against *Plasmodium falciparum* both in vitro and in vivo.²⁰



Fig. 1 (A) *Lantana camara* leaf and (B) synthesized silver nanoparticle

This indicates the synthesis of silver nanoparticles, which was further confirmed by UV-visible spectroscopy. Fig. 2 shows the UV-Vis spectra of the reaction medium after 5 hours. Silver nanoparticles formed in the reaction medium after 5 hours possess maximum absorbance at 430 nm.²³ After a reaction time of 5 hours, peak broadening at 430 nm is observed. This specifies that the particles are poly-dispersed. For optimization reaction parameters, various % of leaf extract and silver solution concentration were taken. Initially 5% leaf extract was added to four different concentrations (2, 3, 4 and 5mM) of silver nitrate solution medium.

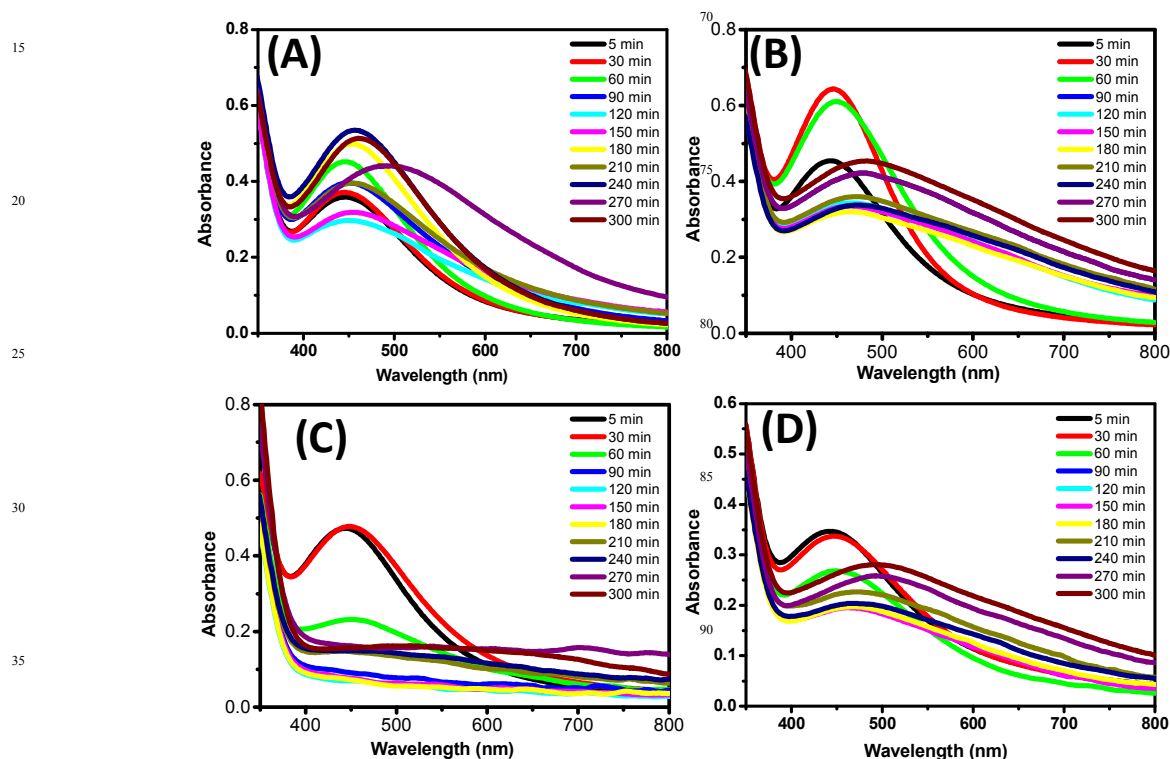


Fig. 2 UV-Visible spectra measurement of Silver nanoparticles synthesis at different conc. of AgNO_3 . (A) 2 mM AgNO_3 solution (B) 3 mM AgNO_3 solution (C) 4 mM AgNO_3 solution (D) 5 mM AgNO_3 solution

In this manuscript we report, a green route for synthesizing silver nanoparticles using *Lantana camara* leaf extract (polyphenol), which acts as both, the reducing and stabilizing agent.²¹ Earlier, *Lantana camara* extract had been used for Ag^0 nanoparticles synthesis,²² while this is the report aimed at its application towards size-controlled green synthesis of Ag^0 nanoparticles.

Result and Discussion

It is well known that the aqueous solution of silver nanoparticles appears yellowish brown because of silver nanoparticles' surface plasmon in the excited state. The addition of leaf extract to the aqueous solution of silver ions (AgNO_3 aqueous solution) results gradual change in the colour of the solution (from slightly green to yellowish) which indicates the reduction of silver ions (Ag^+) and the formation of silver nanoparticles (Ag^0) (Fig. 1B).

Out of four different AgNO_3 solution applied for nanoparticle synthesis, in the case of 3 mM conc., Ag^0 nanoparticles synthesis was observed in just 30 minutes as can be seen in Fig. 2 B. Based on our result we can say that 3mM conc. of AgNO_3 solution is best for better shape control and quick nanoparticle synthesis. Second parameter was optimized by keeping 3 mM silver solution as constant and varying % leaf extract (1, 5, 10 and 20 %). Fig. 3 shows that 10 % leaf extracts demonstrated best results out of four different concentrations used.²⁴ Therefore based on above result, it was observed that 3mM AgNO_3 solution and 10 % leaf extract was the most suitable combination for size controlled Ag^0 nanoparticles synthesis. The morphology and formation of Ag^0 nanoparticles (3mM AgNO_3 solution and 10 % leaf extract) using *Lantana camara* leaf extract was further studied by characteristic absorption bands in FTIR spectrum, X-Ray diffraction pattern, DLS, Zeta-potential scanning and transmission electron microscope images.²⁵

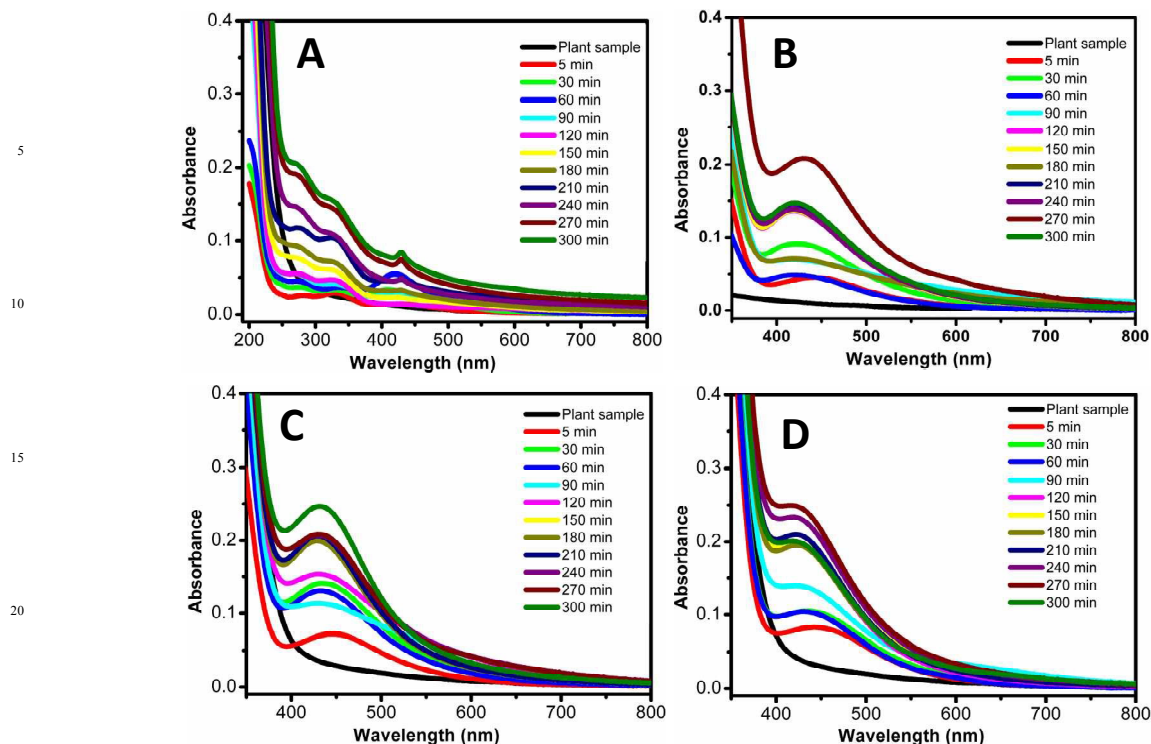


Fig. 3 UV –Visible spectra measurement of Silver nanoparticles synthesis at different percent of leaf extract. (A) 1% leaf extract. (B) 5% leaf extract. (C) 10% leaf extract. (D) 20% leaf extract

Fig. 4 (A) shows FTIR absorption spectra of water soluble leaf extract and Ag^0 nanoparticle. Major absorbance peaks of leaf extract were observed at 1074, 1260, 1432, 1597 cm^{-1} . All above absorbance peaks are associated with the stretching vibrations for C–O (polyols), C–O (esters, ethers) –C C–C O, –C–C– [(in-ring) aromatic], and –C C– [(in-ring) aromatic] respectively.²⁶ Absorption peak at 1260 cm^{-1} appear due to the presence of C–O group of polyols. It is well known that polyols are mainly accountable for the reduction of Ag^+ ions.

Contribution of polyol groups for Ag^0 synthesis is verified by complete disappearance of this band in FTIR spectrum after the Ag^+ ions bio-reduction. The oxidation of polyol groups to unsaturated carbonyl groups leads to a broad peak at 1640 cm^{-1} because of Ag^+ ions reduction.

The study of crystalline nature and particles size analysis of as synthesized Ag^0 nanoparticles was carried out by X-ray diffraction (XRD). The XRD exhibits peaks corresponding to the face centered cubic structure of Ag^0 nanoparticles (Fig.4 B).

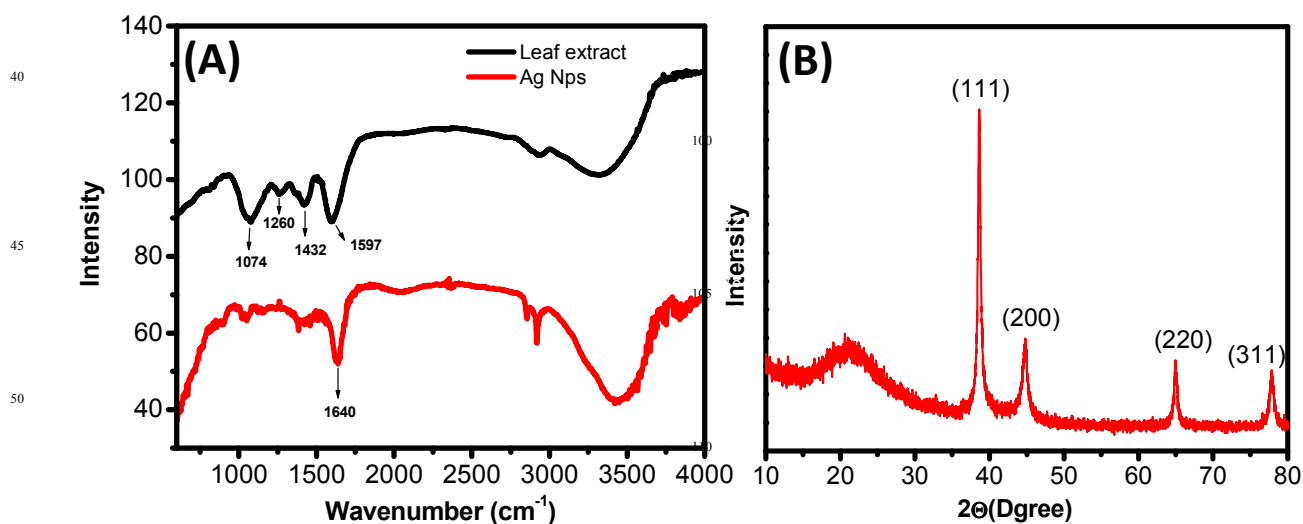


Fig. 4(A) FTIR spectrum of leaf extract and as synthesized Ag^0 nanoparticles. A peak at 1640 cm^{-1} indicates the formation of Ag^0 nanoparticles. **(B)** XRD spectra of Ag^0 nanoparticles. 2θ peaks values at 38.06 θ , 43.56, and 64.37, and 77.24 correspond to (111), (200), (220) and (311) planes, respectively.

20 peaks values at 38.06, 43.56, and 64.37, and 77.24 correspond to (111), (200), (220) and (311) planes, respectively.²⁷ X-ray diffraction pattern confirms that the Ag⁰ nanoparticles formed by the reduction of Ag⁺ ions through *Lantana* leaves extract are nano-crystalline in nature. Average size of Ag Nps calculated from XRD data by applying Debye-Scherrer equation is $\sim 40 \pm 2.8$ nm.

Stability of Ag⁰ nanoparticles was measured by using zeta potential measurement. The zeta potential states the electrical potential on nanoparticle boundary and can be used to determine the nanoparticle surface charge. The zeta potential value for this sample was -36.61 mV.²⁹ Zeta potential value of -36.61 mV in solution state is considered as excellent to prevent agglomeration; hence were highly stable.

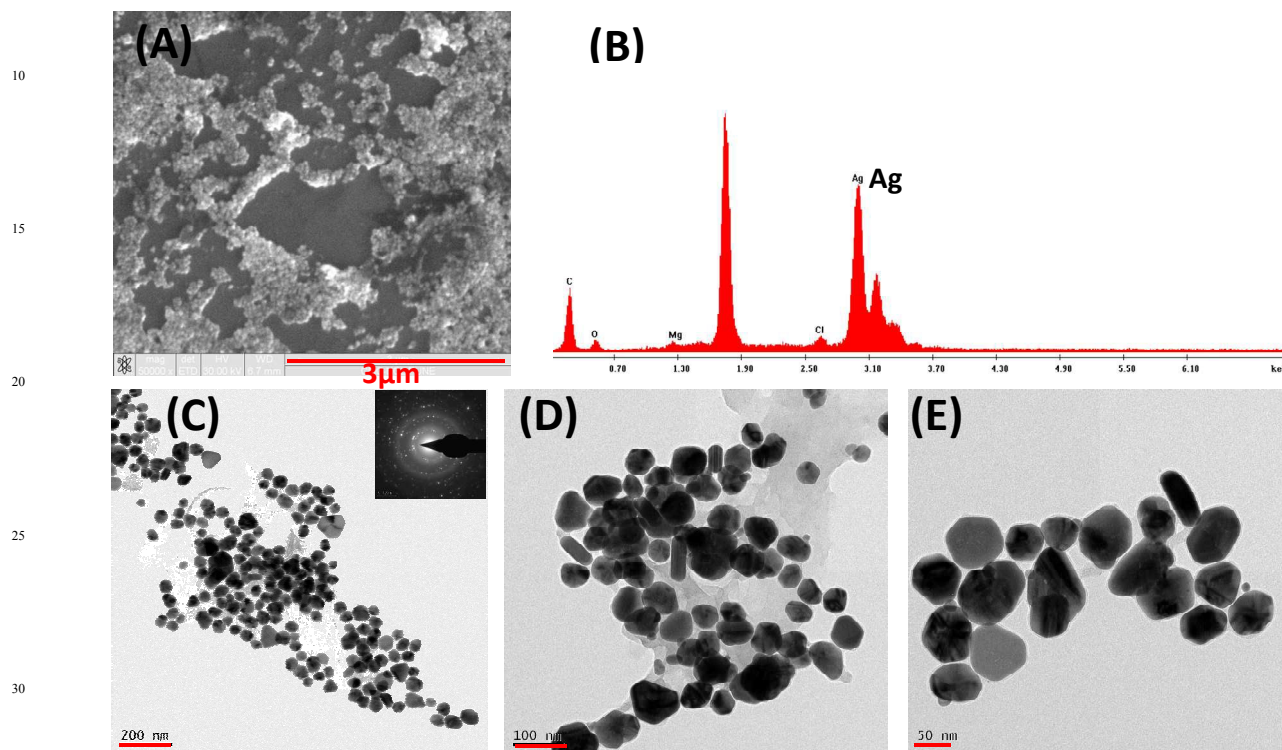


Fig. 5 (A) SEM image of Ag⁰ nanoparticles (B) Edax spectra of Ag⁰ nanoparticles SEM image. TEM images of Ag⁰ nanoparticles for better resolution of morphological studies at different scale bar. (C) (200 nm) (D) (100 nm) and (E) (50 nm).

Ag⁰ nanoparticles sample was further examined by scanning electron microscopy (SEM). Ag⁰ nanoparticles appear as organized large assembly due to the resolution limitation of SEM (Fig. 5A). Edax analysis of Ag⁰ nanoparticles SEM shows presence of Ag⁰ (Fig. 5B). The organized large assembly of Ag⁰ nanoparticles in SEM evolves due to solution drying process and do not represent the situation in the solution. To better understand the morphologies of Ag⁰ nanoparticles transmission electron microscopy (TEM) was performed (Fig. 5 C-E) that illustrate the round and rod-needle type shape anisotropy. Fig 5 C (inset) demonstrates the diffraction pattern of TEM image which evident of crystalline nature of Ag⁰ nanoparticles (identical with XRD). As seen in Fig. 5 D, a thin layer of *Lantana* leaf extract surrounds the Ag⁰ nanoparticles surface, adding to its stability.²⁸

Hydrodynamic radius of Ag⁰ nanoparticles was analyzed at a constant shutter opening diameter in the DLS apparatus. DLS measurements for Ag⁰ nanoparticles exhibit hydrodynamic radii of about ~ 41.8 nm (Fig. 6 A). This hydrodynamic radius was also confirmed by analysis of XRD and TEM results. Polydispersity index of Ag⁰ nanoparticles in DLS experiment was 0.297, which is considered as excellent for their biomedical applications.

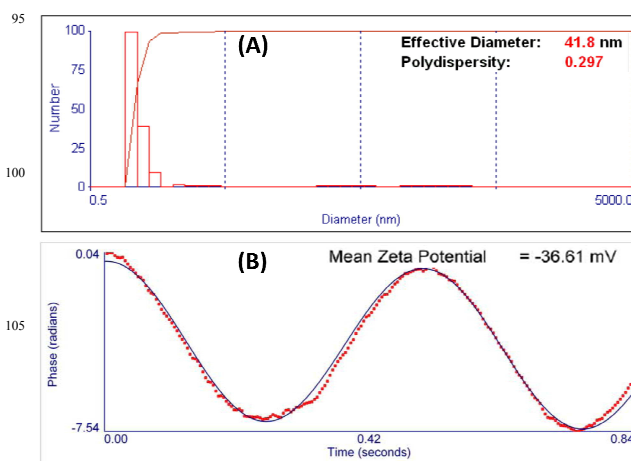


Fig. 6 (A) DLS and Zeta Potential results for Ag Nps showing hydrodynamic radius of ~ 41.8 nm and (B) zeta potential value of Ag Nps showing -36.61 mV.

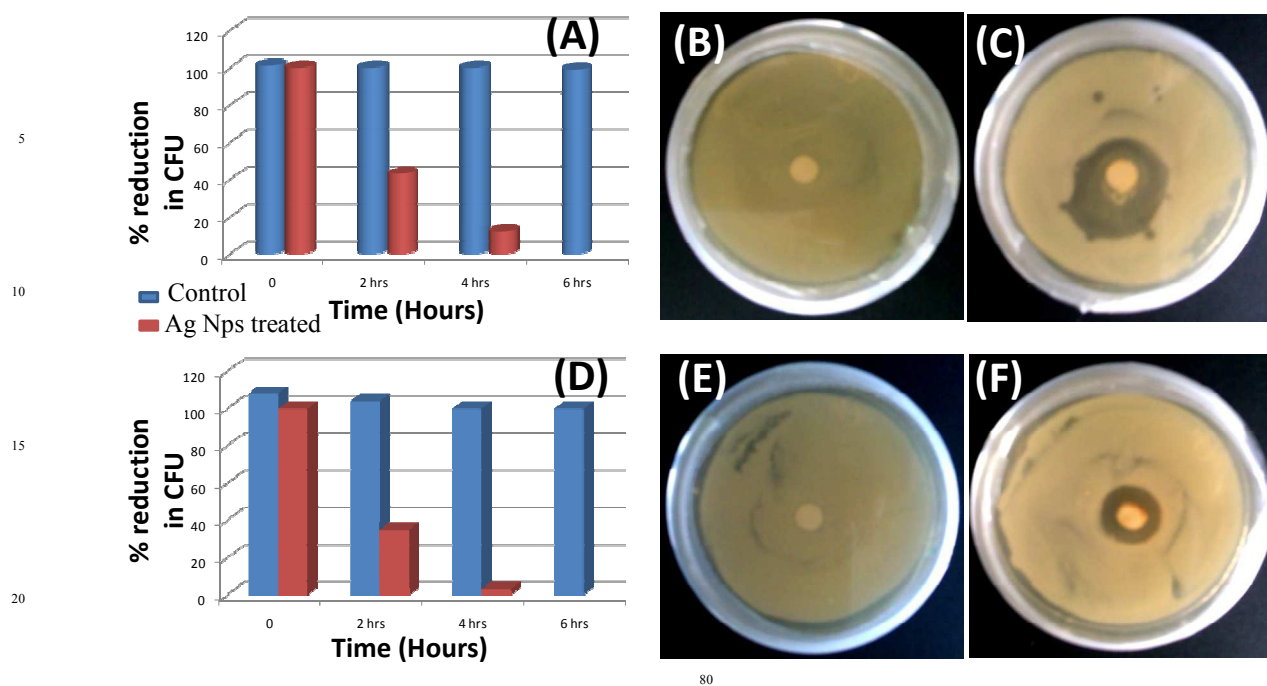


Fig. 7 Ag⁰ nanoparticle antibacterial activity against *E. coli* and *S. aureus* as it showed by contact inhibition method (A) *E. coli* control and *E. coli* cells treated with 50 ppm Ag⁰ nanoparticle (B) *E. coli* control plate (C) *E. coli* plate with Ag⁰ nanoparticle (D) *S. aureus* control and *S. aureus* treated with 50 ppm Ag⁰ nanoparticle. (E) *S. aureus* control plate (F) *S. aureus* plate with Ag⁰ nanoparticle

These Ag⁰ nanoparticles synthesized by green approach were found to be extremely toxic to two pathogenic multidrug resistant bacteria (*E. coli* and *S. aureus*).

Lowest concentration of compound which inhibits the visible growth of microbes on the culture plate is called minimum inhibitory concentration (MIC). Initially the minimum inhibitory concentration (MIC) of Ag⁰ nanoparticles was studied by treating both the microorganisms with different concentrations (10, 20, 30, 40, 50, 60, 70, 80, 90, 100 ppm) of Ag nanoparticles.

Minimum inhibitory concentrations of Ag nanoparticles were determined on both bacterial cultures. Optical density of both bacterial suspensions was measured at 600 nm wavelength, and same absorbance of bacterial suspension was fixed and preserved throughout the process. MIC against *E. coli* was found to be 50 ppm, whereas it was 60 ppm for *S. aureus*.

Based on the MIC concentration, antibacterial activity of Ag⁺ nanoparticles was performed on both the bacterial culture, which shows that it took 6 hours for the complete inhibition in contact mode method (Fig. 7 A, D). Antibacterial effects of Ag⁰ nanoparticle obeyed zone growth inhibition action mechanism over both bacterial cell cultures. Control plates of both bacterial cultures showed no inhibition zone (Fig. 7 B, E), whereas Ag⁰ nanoparticle loaded disk exhibited antibacterial activity against *E. coli* and *S. aureus* (Fig. 7 C, F) respectively.

Fig 8 shows the SEM images of the both bacterial cells culture treated with Ag⁰ nanoparticle. Control *E. coli* cells (without Ag⁰ nanoparticles) are illustrated in Fig. 8 (A, C) expressing clear defined bacterial morphology.³¹

Ag⁰ nanoparticles treated *E. coli* cells show a damage undefined cellular morphology. Effect of the Ag⁰ nanoparticles on the *E. coli* cell membrane damage and releasing cellular contents are confirmed by SEM image (Fig. 8 B, D). Fig. 8 C and D shows the resolution SEM images of Fig 8 A and B for better understanding of the effect of Ag⁰ nanoparticles on bacterial cell morphology. When *E. coli* cells come in contact with Ag⁰ nanoparticles they damage *E. coli* cell membrane resulting in the excretion of the cellular components. Cellular content of *E. coli* cells can be clearly seen in Fig 8 D.³²⁻³³

Antibacterial activity of Ag⁰ nanoparticles was observed on gram (+) bacteria *S. aureus*. Fig 8 E exhibits the control *S. aureus* cells while Fig. 8 F shows the Ag⁰ nanoparticles antibacterial effect. Fig 8 (G) and (H) illustrated the resolution SEM image of Fig 8 (E) and (F) respectively. Both bacterial cell membranes are found to be damaged and extracellular material released.³⁴ The consequences of damaged cell membrane integrity might be due to the formation of membrane pores leading to leakage of cytoplasmic contents and accumulation of cell debris were also noted (red circle in Fig 8 B, D and F, H).

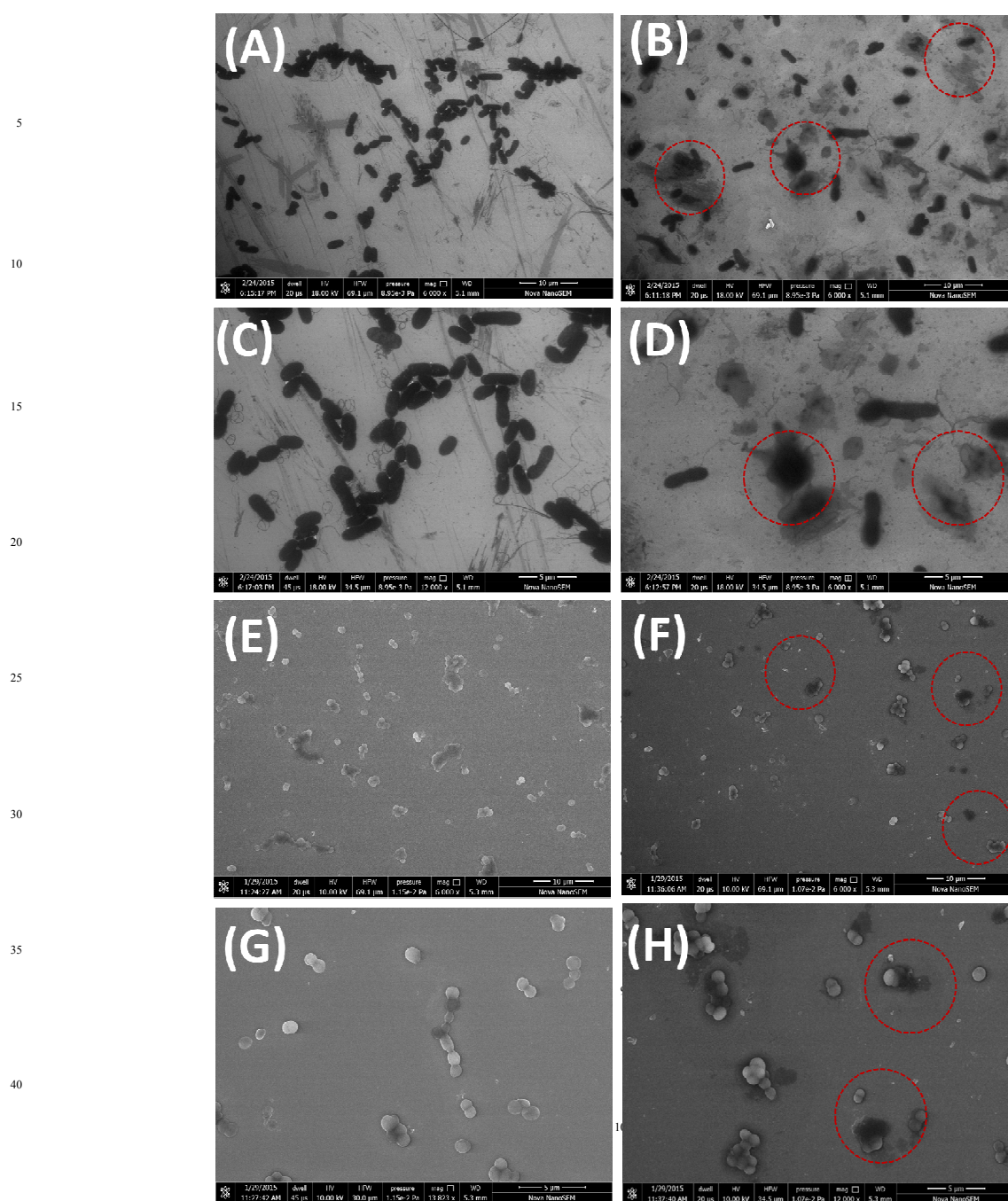


Fig. 8 SEM images of both control bacterial cell cultures and with Ag^0 nanoparticle treated bacterial cell culture morphology. (A) control *E. coli* cells (B) Ag^0 nanoparticle treated damaged *E. coli* cell (C-D) resolution images of A and B respectively (E) control *S. aureus* cells (F) Ag^0 nanoparticle treated damaged *S. aureus* cell. (G-H) resolution images of C and D respectively. Red circle in SEM images shows the release of bacterial cell content after Ag^0 nanoparticle antibacterial action (Scale bar $10\mu\text{m}$ (A, B, E and F) and $5\mu\text{m}$ (C, D, G and H))

Conclusion

Leaf extract of the *Lantana camara* plant has been reported for the bio-reduction of aqueous Ag^+ ions to Ag^0 metal ions which lead to the formation of well-defined Ag^0 nanoparticles. Size control of nanoparticles has been done by analysing various concentrations of silver solution and leaf extract. UV-Vis, FTIR spectroscopy, XRD, SEM and TEM analysis was used to investigate shape and size control of nanoparticles.

Analysis of FTIR spectra shows that the polyols present in leaf extract are responsible for reduction of Ag^+ ions to Ag^0 nanoparticles synthesis. Particle size of nanoparticle around ~ 41.8 nm was confirmed by XRD, DLS, and zeta-potential analysis as well as by TEM images. Green synthesized Ag^0 nanoparticle show excellent antibacterial activity against gram (+) and gram (-) bacteria at fairly low concentration.

Materials and Methods

Plant material and preparation of the leaf extract

Lantana camara's aqueous leaf extract was used for nanoparticle synthesis. 25g leaves of *Lantana camara* were weighed and thoroughly washed in distilled water to remove dirt and other adherent material. Then the leaves were crushed and boiled in 100 ml distilled water for 10 minutes. After it was cooled to room temperature, filtered using Whatman filter paper 1 (pore size 25 μm) followed by 0.45 μm syringe filter. Filtrate solution was referred as stock solution and used directly of Ag^0 nanoparticles synthesis.

Synthesis of Silver Nanoparticle

2-5 mM Silver nitrate (AgNO_3) aqueous solution was prepared for the synthesis of silver nanoparticles. *Lantana camara* leaf extract at varying concentration from 1% to 20% v/v was added to silver nitrate solution at room temperature and incubated for 5 hours. Reduction of Ag^+ ions to Ag^0 nanoparticles into size controlled nanoparticles was optimized by varying the concentration of silver nitrate aqueous solution from 2 mM to 5 mM.

UV-Visible Spectra analysis

Synthesis of Ag nanoparticles was monitored by recording the UV-Visible spectrum at different time interval of the reaction medium. Samples were diluted into distilled water before measuring UV spectra. 10 mm quartz cell at 25 ± 0.1 $^\circ\text{C}$ was used for UV-Vis spectral analysis on Varian CARY 100 Bio UV-Vis spectrophotometer. Appropriate controls were used wherever required.

FTIR measurement

The unreacted biomass filtrate was removed by centrifuging 100 mL of residual solution after synthesis at 5000 rpm for 10 minutes. Then 10 mL sterile distilled water was used for making final sample suspension. Washing process mentioned above was repeated thrice. Subsequently, the final suspension was freeze dried to powder and analysed by FTIR.

SEM and TEM analysis of silver nanoparticles

Field emission scanning electron microscopy images were acquired on FEI QUANTA 200 microscope, equipped with a tungsten filament gun, operating at WD 10.6 mm and 20 kV. The samples were dried overnight at room temperature and images were recorded without gold coating. TEM measurements were performed on Tecnai F 30 instrument operated at an accelerating voltage of 300 kV. Fine films of the nanoparticles were prepared by drop casting method on a carbon coated copper grid.

DLS measurements

DLS measurements were carried out on Brookhaven Instrument model 90 Plus Particle Size Analyzer.

Zeta Potential

The surface charges of the Ag Nps were determined using a Zeta potential analyzer (Brookhaven Instruments Corporation, NY). The average Zeta potentials of the dispersions were determined without any dilution.

Antibacterial assays

The minimum inhibitory concentration (MIC) and antibacterial assays were performed on *Escherichia coli* (ATCC 8739) and *Staphylococcus aureus* (ATCC 6358) by contact and disc diffusion method. Both the microorganisms were grown in Luria Bertani (LB) medium. A contact mode inhibition method assures positive interaction between silver nanoparticles and bacteria. Silver nanoparticles were added into bacterial suspension (10^4 - 10^6 CFU/ml) and incubated at 30 $^\circ\text{C}$ for 6 h. 100 μl sample was withdrawn after every 2 h to check viability of bacteria. To calculate minimum inhibitory concentration (MIC), different concentration of Ag^0 nanoparticles were added to $\sim 1 \times 10^5$ cells/mL (*E. coli* and *S. aureus* respectively) and incubated at 28 $^\circ\text{C}$. Defined amount of aliquots were removed at different time interval (0, 2, 4, 6, 8, 10 hrs) and plated on nutrient agar, incubated at 28 $^\circ\text{C}$ for 18-24 hrs to achieve visible colony forming units. For checking zone of inhibition, overnight grown inoculums of both cultures (5×10^6 CFU mL^{-1}) were applied on plate of LB agar respectively. 6 mm diameter size discs of sterile whatman paper were loaded with $50 \mu\text{g/mL}$ (50 ppm) silver nanoparticle and placed on previously seeded bacterial culture respectively.

Acknowledgement:

This work is financially supported by the Council of Scientific and Industrial Research, New Delhi India.

Notes and references:

- S. Agnihotri, S. Mukherji and S. Mukherji, RSC Advances **4** (8), 3974-3983 (2014).
- J. L. Gardea-Torresdey, E. Gomez, J. R. Peralta-Videa, J. G. Parsons, H. Troiani and M. Jose-Yacaman, Langmuir **19** (4), 1357-1361 (2003).
- S. Irvani, Green Chemistry **13** (10), 2638-2650 (2011).
- P. Raveendran, J. Fu and S. L. Wallen, Journal of the American Chemical Society **125** (46), 13940-13941 (2003).
- U. K. Parashar, V. Kumar, T. Bera, P. S. Saxena, G. Nath, S. K. Srivastava, R. Giri and A. Srivastava, Nanotechnology **22** (41) (2011).
- I. Ahmad and A. Z. Beg, Journal of Ethnopharmacology **74** (2), 113-123 (2001).
- W. Ding and X. P. Hu, Insect Science **17** (5), 427-433 (2010).
- S. S. Shankar, A. Ahmad, R. Pasricha and M. Sastry, Journal of Materials Chemistry **13** (7), 1822-1826 (2003).
- B. Ankamwar, C. Damle, A. Ahmad and M. Sastry, J Nanosci Nanotechnol **5** (10), 1665-1671 (2005).
- J. L. Huang, Q. B. Li, D. H. Sun, W. Y. Shao, N. He, J. Q. Hong and C. X. Chen, Nanotechnology, **18** (10) (2007).
- Z. L. Xue, A. D. Terepka and Y. Hong, Nano Letters, **4** (11), 2227-2232 (2004).

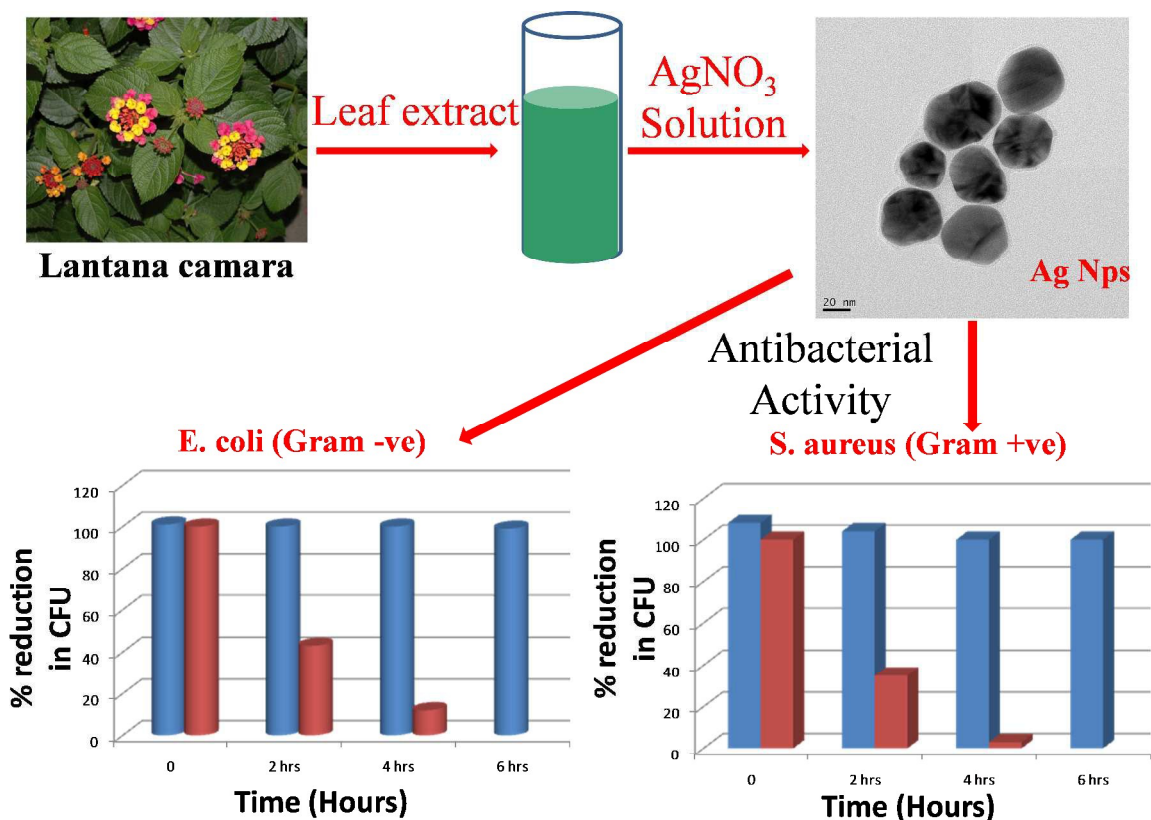
- 12 . N. R. Jana, L. Gearheart and C. J. Murphy, *Advanced Materials* **13** (18), 1389-1393 (2001).
- 13 T. M. d. A. Alves, A. F. Silva, A. Smânia Júnior, C. L. Zani, *Memórias do Instituto Oswaldo Cruz*, **95**, 367-373 (2000).
- 14 A. S. Shaikat and I. A. Siddiqui, *Phytopathol. Mediterr.* (2001) **40**, 245–25
- 15 S. S. Shankar, A. Ahmad, M. Sastry, *Biotechnology Progress* **19** (6), 1627-1631 (2003).
- 16 N. Misra, M. Sharma, K. Raj, A. Dangi, S. Srivastava and S. Misra-Bhattacharya, *Parasitology Research* **100** (3), 439-448 (2007).
- 17 S. Begum, A. Wahab, B. S. Siddiqui, F. Qamar, *Journal of Natural Products* **63** (6), 765-767 (2000).
- 18 B. M. Pour, L. Y. Latha, S. Sasidharan, *Molecules* **16** (5), 3663-3674 (2011).
- 19 J. Carrión-Tacuri, A. E. Rubio-Casal, A. de Cires, M. E. Figueroa, J. M. Castillo, *Photosynthetica* **49** (3), 321-329 (2011).
- 20 R. Geethalakshmi, D. V. L. Sarada, *International Journal of Nanomedicine* **7**, 5375-5384 (2012).
- 21 R. Pala, R. Pathipati Usha, S. Bojja, *Journal of Nanoparticle Research* **12** (5), 1711-1721 (2010).
- 22 D. Kumarasamyraja, N S Jeganathan, *Int. Res. J. Pharmacy*, 2013, **4** (5), 203-207
- 23 C. Jayaseelan, A. Rahuman, G. Rajakumar, A. Zahir and G. Elango, *Parasitology Research* **109** (1), 185-194 (2011).
- 24 P. Mukherjee, A. Ahmad, R. Kumar and M. Sastry, *Nano Letters* **1** (10), 515-519, 2001.
- 25 P. K. Jain, K. S. Lee, I. H. El-Sayed and M. A. El-Sayed, *The Journal of Physical Chemistry B* **110** (14), 7238-7248 (2006).
- 26 K. B. Narayanan and N. Sakthivel, *Materials Letters* **62** (30), 4588-4590 (2008).
- 27 H. Bar, D. K. Bhui, A. Misra, *Colloids and Surfaces A: Physicochemical and Engineering Aspects* **339** (1–3), 134-139 (2009).
- 28 J. Zhang, M. R. Langille and C. A. Mirkin, *Nano Letters* **11** (6), 2495-2498 (2011).
- 29 S. Marimuthu, A. Rahuman, G. Elango and C. Kamaraj, *Parasitology Research* **108** (6), 1541-1549 (2011).
- 30 K J-Navare, A Prabhune, *BioMed Res Int. Volume* 2013, Article ID 512495, 8 pages
- 31 C Jayaseelan, A A Rahuman, G Elango, *Parasitol Res.* 2011, Jul, **109**, 185-94.
- 32 M Saravanan, A Nanda, *Colloids and Surfaces B: Biointerfaces*, **77**, 214–218, (2010)
- 33 M Saravanan, A K Vemu, S K Barik, *Colloids and Surfaces B: Biointerfaces*, **88**, 325-331, 2011
- 34 P Prakash, P Gnanaprakasam, M. Saravanan, *Colloids and Surfaces B: Biointerfaces*, **108**, 255-259, 2013

Table of Contents

Textual Abstract

Ag⁰ nanoparticles were synthesized by *lantana Camara* plant (weed) leave extract. Antibacterial activity of as synthesized Ag⁰ nanoparticles was excellent against both Gram –ve and Gram +ve bacterial culture.

Graphical Abstract



Ag Nps were synthesized by *lantana Camara* plant (weed) leave extract. Antibacterial activity of as synthesized Ag Nps were excellent against both Gram –ve and Gram +ve bacterial culture.